

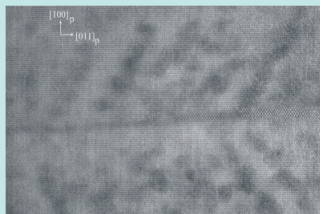
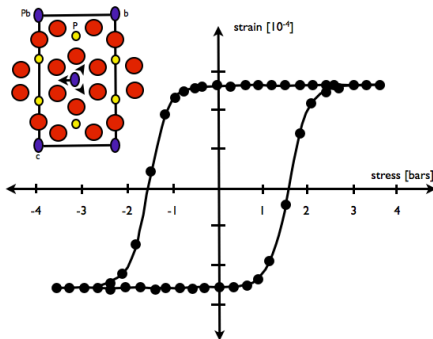
Domain boundary engineering in (multi-) ferroics -experiments-

*Ekhard Salje
University of Cambridge*

Salje EKH. 2010. Multiferroic domain boundaries as active memory devices: trajectories towards domain boundary engineering. *ChemPhysChem* 11:940--50

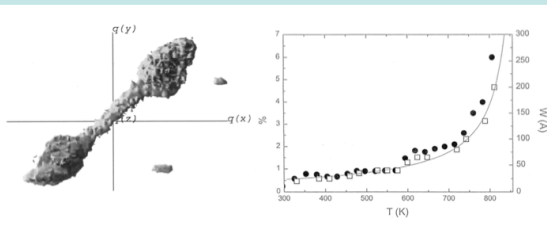
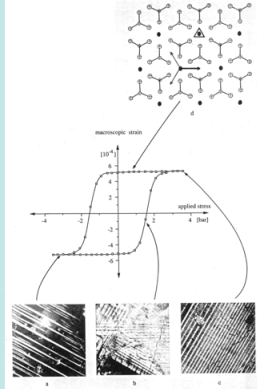
Salje EKH 1993 Phase Transitions in ferroelastic and co-elastic crystals Cambridge University Press , Cambridge UK

Van Aert S, Turner S, Delvill R, Schreyvers D, Van Tendeloo G, Salje EKH 2012
Direct observation of ferroelectric domain boundaries in CaTiO₃ by electron microscopy
Advanced Materials 34: 523-527



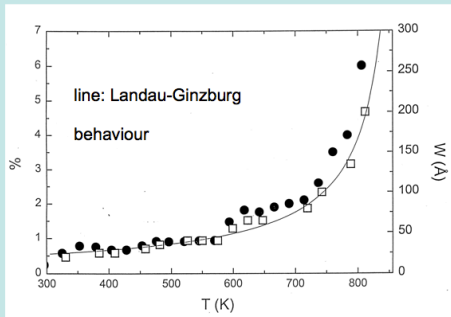
Typical wall thickness in perovskites at $T \ll T_c$ is $> 2\text{nm}$

twin walls can be generated easily and twin walls can be moved by external stresses. This allows the formation of specific patterns according to applications.



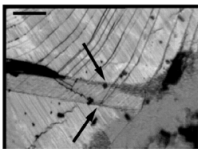
diffraction to measure the thickness of interfaces

5

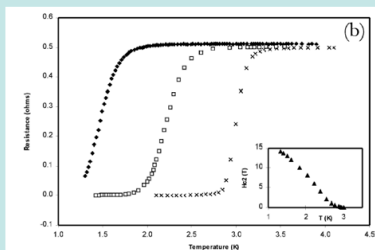


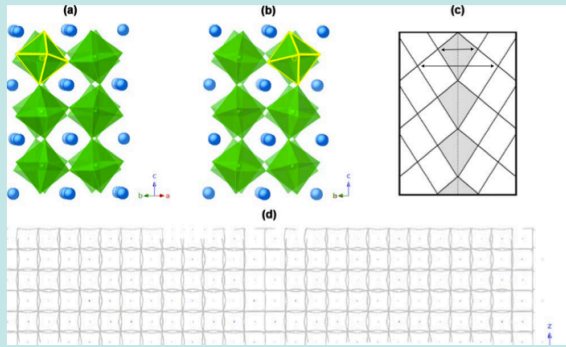
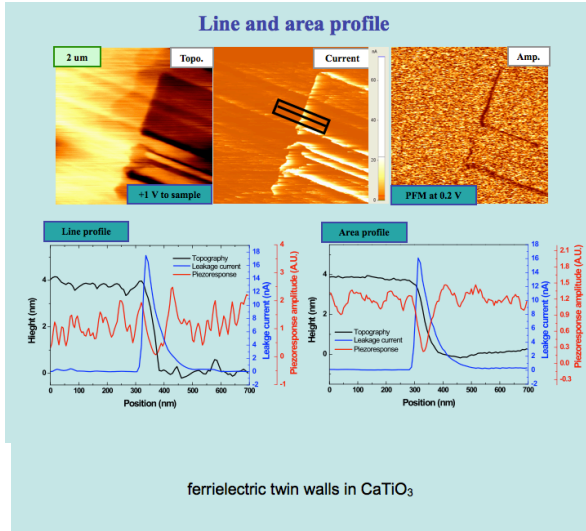
Temperature evolution of the wall thickness in LaAlO_3

(Chrosch & Salje, JAP 1999)

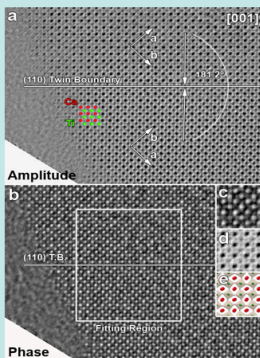
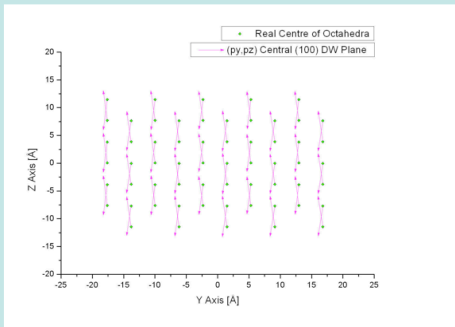


Supercurrents along twin boundaries in WO_3



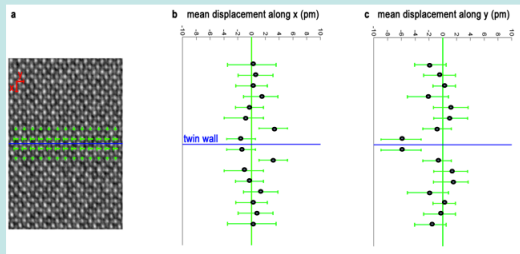


CaTiO₃ ferroelectric and anti-ferroelectric distortion in ferroelastic twin walls



CaTiO₃

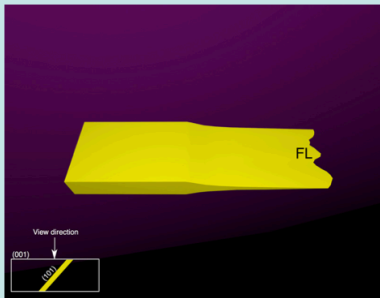
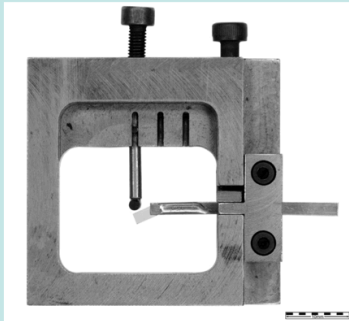
Titan TEM reconstructions for amplitude and phase (2012) in press



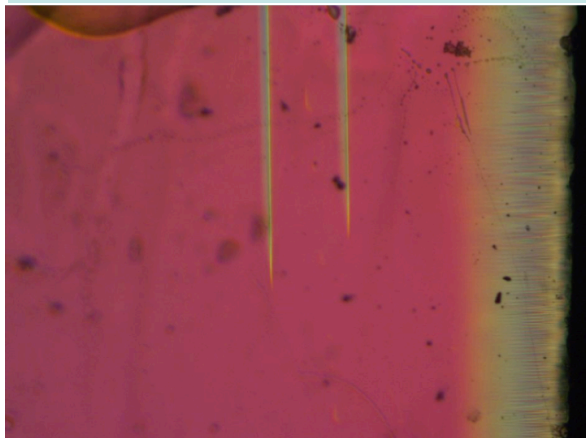
Ti atoms are shifted to the left, amplitude ca. 6pm
no shifts for Ca beyond the thermal noise level

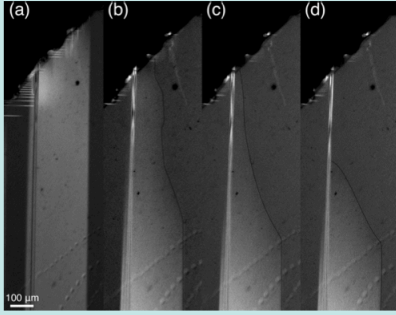
13

quasi-static shear experiment

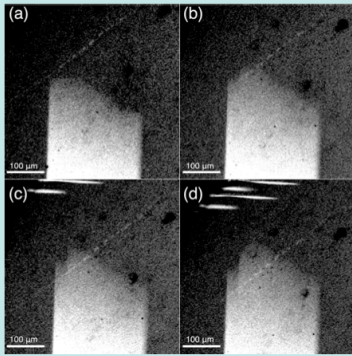


16

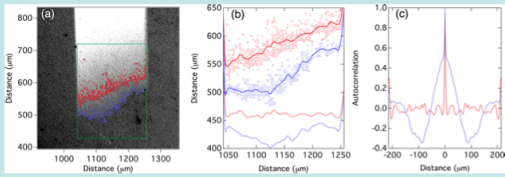




18



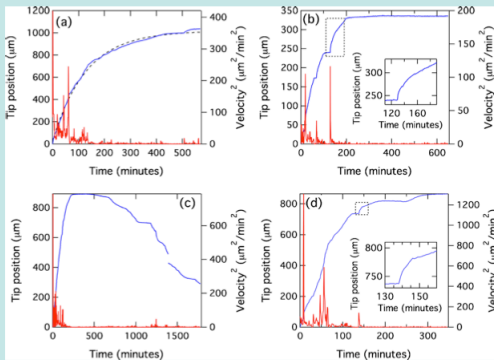
19

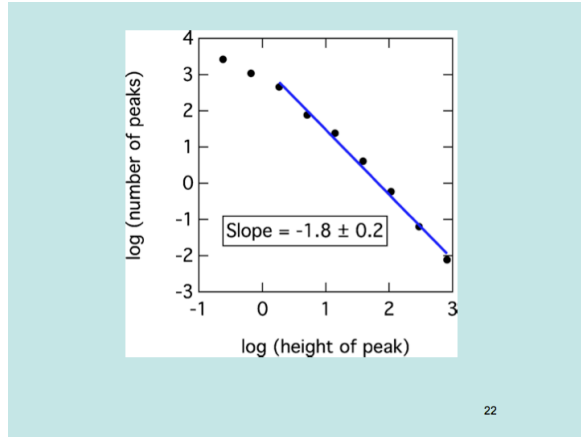


the front line defines the Larkin length while the Larkin length of the surface planes remains infinite

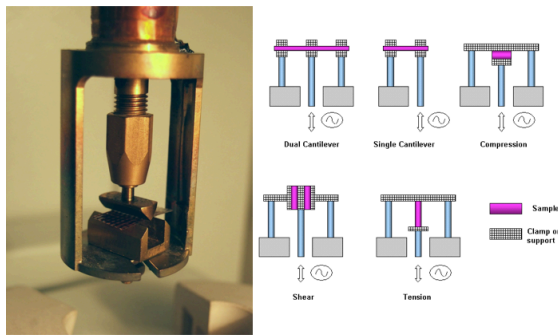
20

Jerky propagation and energy spectrum

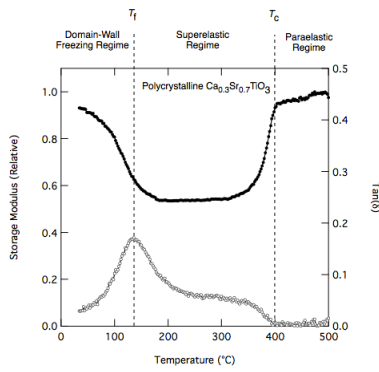




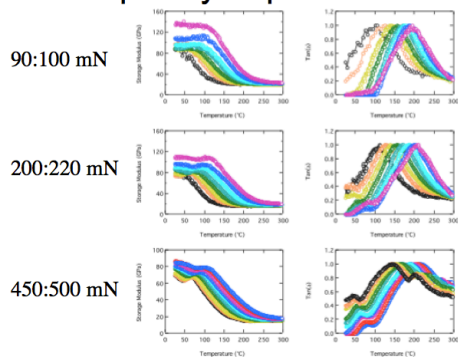
22



dynamical mechanical analyzer (0.01 - 30 Hz)



Frequency-dependence



Elastic response function

- $J(t) = \epsilon(t)/\sigma = J_{\text{unrelaxed}} + \Delta J(1 - \exp(-t/\tau))$

$$J(\omega) = J_{\text{unrelaxed}} + \Delta J / (1 + i\omega\tau) \quad \text{Debye}$$

- Extended Debye

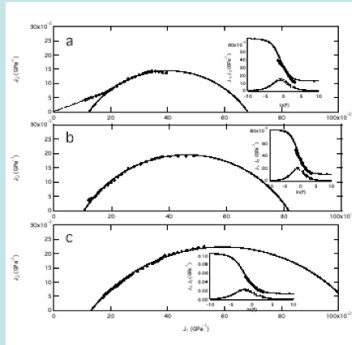
$$J(\omega) = J_{\text{unrelaxed}} + \Delta J / (1 + i\omega\tau)^\mu$$

- Equivalent to density function in τ

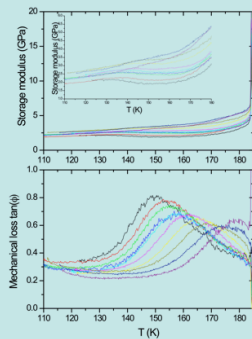
$$\rho(\tau) = (\tau^{\mu-1} \sin(\mu\pi) / \pi) / (1 + \tau^{2\mu} + 2\tau^\mu \cos(\mu\pi))$$

- First moment $\tau\rho(\tau)$ gives the probability function of τ

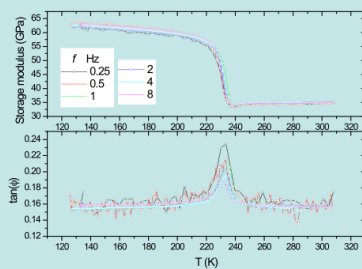
Elastic Cole-Cole plots: 'flattened' semicircles



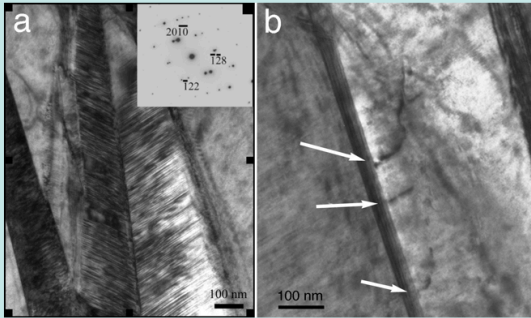
'standard' elastic softening by mobile walls in KMnF_3



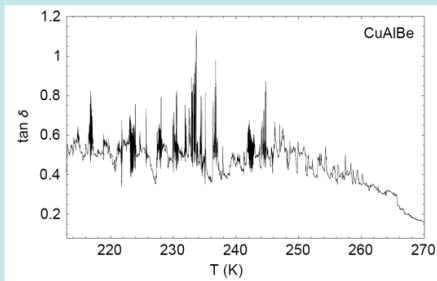
Mobile interface austenite/martensite but no mobility martensite/martensite



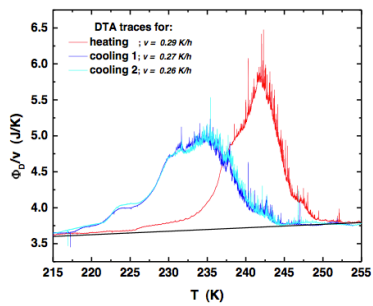
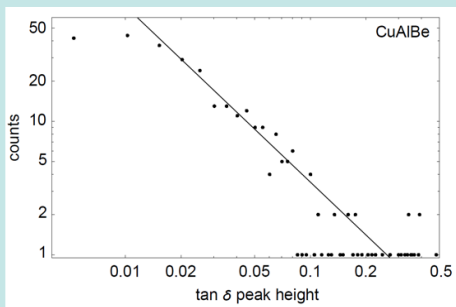
Dislocations nucleating in a twin wall in CuAlBe



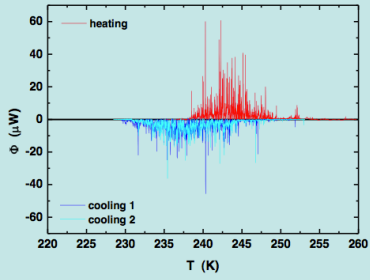
Avalanches in martensites
(Salje et al. APL 2009)



Power law for avalanches ($\tau = 1.3$)

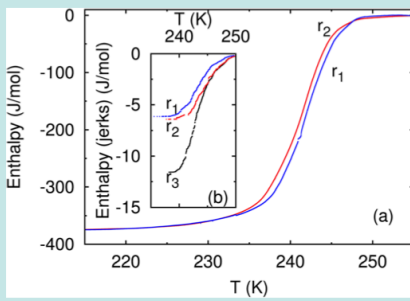


CuAlZn

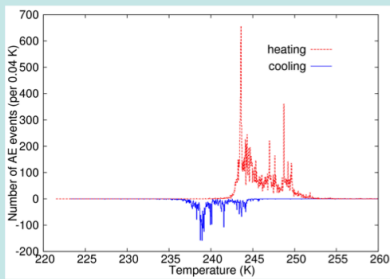


jerk contribution

35

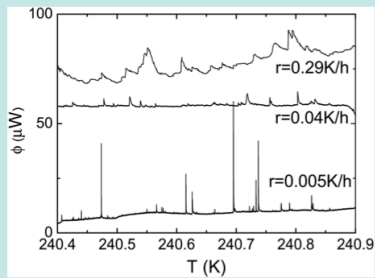


36

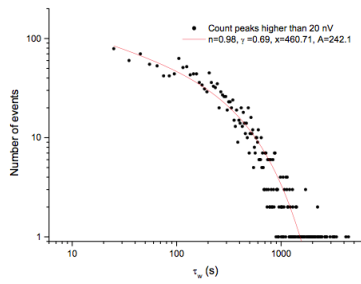
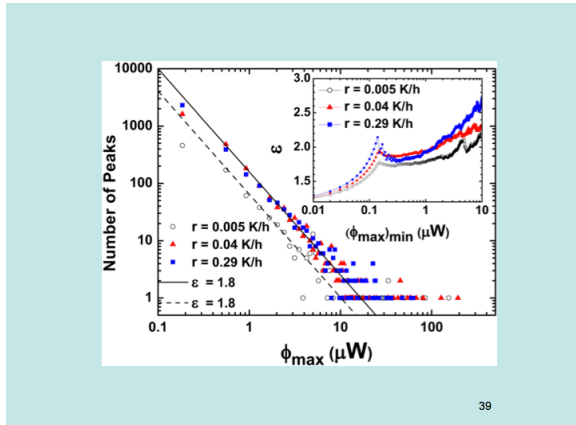


acoustic emission

37



38

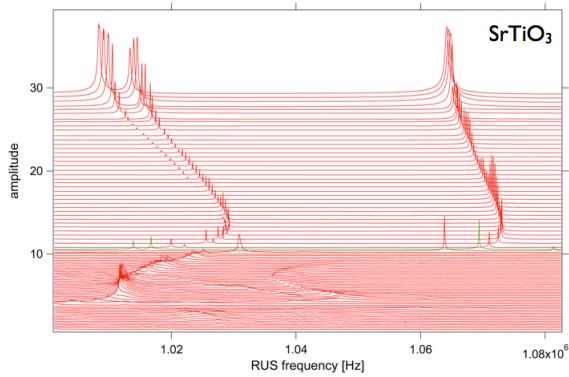


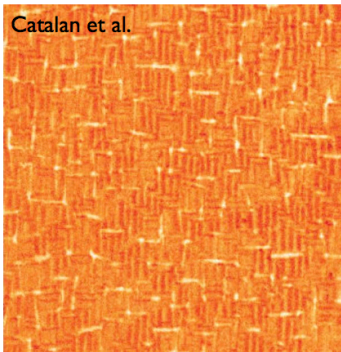
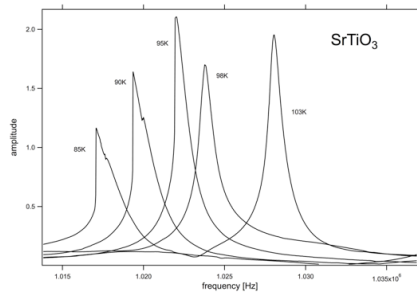
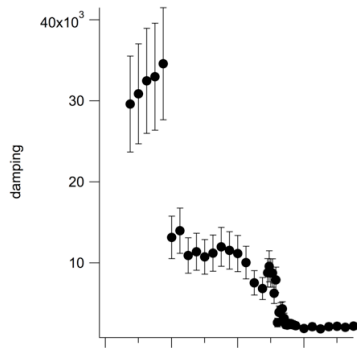
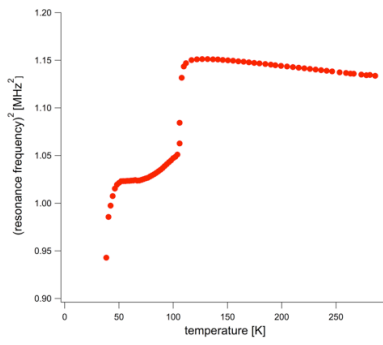
Statistical distribution of the waiting time between jerks.
 The quantitative parameterization of the distribution
 $p(wt) \sim wt^{(\gamma-1)} \exp(-wt/\tau)^n$
 leads to $n=1$, $\gamma=0.7$, and $\tau=460$ s.

41

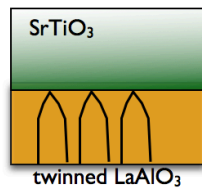


fast (kHz-MHz)
 resonance ultrasonic
 spectroscopy
 RUS

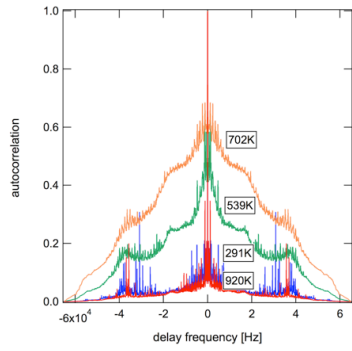
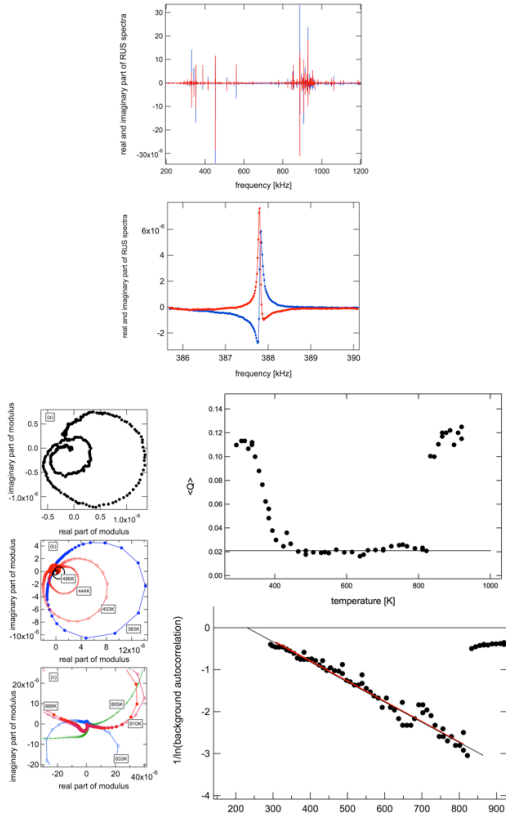




Catalan et al.

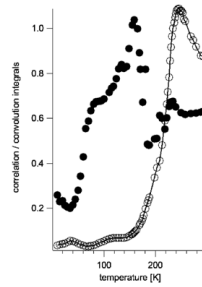


twinning in flexomechanics: here an interface between LaAlO₃ on SrTiO₃



autocorrelation function LaAlO3

magnetic transitions



Temperature evolution of the integral autocorrelation, ψ_i (black circles) and the integrated convolution, λ (open circles)